AIAA 82-4208

Aerodynamic Behavior of a Slender Slot in a Wind Tunnel Wall

Donald B. Bliss*
Princeton University, Princeton, N.J.

A theoretical model for the flow through a single slot of finite length in a wall separating a uniform freestream and a quiescent fluid at different static pressures is constructed. This problem is relevant to understanding the aerodynamic behavior of slots which are used in the test sections of some ventilated wall transonic wind tunnels. The theoretical relationship which is obtained between the pressure differential across the slot and the flow through the slot shows both the linear and quadratic regimes observed in experiments. The linear behavior arises from the acceleration of the cross flow into the slot downstream of the leading edge and from the interaction of streamwise stations along the slot, as well as from the effect of slot taper. Analytical solutions are obtained for two slot planform shapes, and some other cases are solved numerically. The quantitative agreement with experimental data is very encouraging.

Introduction

VENTILATED walls are used in the test sections of transonic wind tunnels in order to reduce blockage effects. In some designs, fluid is allowed to leave or enter the test section through slender slots parallel to the flow which are distributed along the test section walls. The size, aspect ratio, spacing, and other geometric properties of the slots may vary considerably for different tunnels. In order to include wind tunnel wall interference effects in transonic flow calculations the effect of the slots on the wall boundary condition must be included. One step in this direction is to understand the flowfield in the vicinity of a single slot.

The problem to be analyzed is the flow through an isolated finite length slot in an infinite wall separating a uniform freestream and a quiescent fluid at different static pressures. Other than the effect of the slot there are assumed to be no other nonuniformities in the flowfield. This slot flow is illustrated in Fig. 1, where the flow is shown leaving the test section. An experimental plot of pressure difference across a constant width (untapered) slot in uniform flow as a function of the mean velocity through the slot is shown in nondimensional form in Fig. 2.[1] When the mean velocity is small the behavior is linear, whereas when the mean velocity is large the behavior is more nearly quadratic. The fact that the data for different Mach numbers collapses reasonably well onto a single curve supports the idea that the behavior of the slot is dominated by the subsonic cross flow and suggests that the slot can be analyzed using slender-body theory. If, instead, the slot were subjected to a nonuniform flowfield, the behavior of the curve would be altered by the imposition of the corresponding nonuniform pressure gradient along the slot length.

Numerous investigators have studied various aspects of the flow through slots analytically and experimentally; Refs. 2-6 provide a representative sample. There is general agreement that the quadratic behavior seen at higher values of mean slot velocity in Fig. 2 is associated with separation of the cross flow as it passes through the slot. The dependence of pressure drop on the square of velocity is the same as that encountered for a jet or an orifice flow, which the cross flow resembles when the pressure differential is large. Perhaps surprisingly, the linear behavior that occurs when the mean slot velocity is small is not as well understood.

Received Nov. 8, 1978; revision received June 25, 1981.

*Assistant Professor, Mechanical and Aerospace Engineering.

It has become common practice to represent a slotted wind tunnel wall by a local boundary condition obtained by averaging over the slotted and solid regions of the wall. In this case the local behavior of a row of slots, rather than an isolated slot, is considered. The boundary condition that is usually presented relates the local pressure differential to a streamline curvature term, and to terms that are linear and quadratic in the normal velocity. Analytical formulas have been proposed for the streamline curvature and quadratic terms, and for the linear term when the slot is tapered[2-4] and when the free surface location is variable within a channel-like slot cross section.[5,6]

Since untapered slots are known to exhibit linear behavior for low mean velocity through the slot, there has been a tendency to assume that the local boundary condition needs another linear term arising from effects other than those just mentioned. Attempts have been made to attribute the linear behavior to a viscous effect in the vicinity of the slot.[1] This explanation appears to be incorrect; in fact, the effect of viscosity is probably to contribute another quadratic term. Another possible explanation is related to the interaction of the flow with the trailing edge of the slot. For instance, a thick blunt trailing edge would cause a flow deflection not unlike that produced by the holes in a perforated wall which are known to have a linear characteristic. However, if this were the mechanism, the slope of the linear region would probably depend on Mach number. Also, slots with thin sharp edges are known to exhibit linear behavior at low mean slot velocities. Berndt,[5] in reviewing the current problems associated with slotted wall wind tunnels, has stated that the ideas which have thus far motivated the inclusion of the additional linear term in the theoretical boundary condition are probably not entirely correct.

The following analysis of an isolated slot contributes to the general understanding of slot flows in wind tunnel walls. The results show that the previously mentioned linear behavior will arise even when the slot is not tapered, and even when the free surface displacement is very small. In other words, the linear behavior occurs even under conditions for which no term involving a linear proportionality between pressure differential and normal velocity would appear in the local averaged boundary condition for a wall covered with slots. Physically, this linear behavior is associated with the convective acceleration of the cross flow into the slot in the region downstream of the leading edge. If the mean flow through the slot is small, the cross flow never reaches its fully developed state and linear effects dominate. When the mean flow is large, most of the cross flow resembles a fully developed jet or orifice flow and the quadratic term dominates. For the linear case, the somewhat analogous situation in classical slender

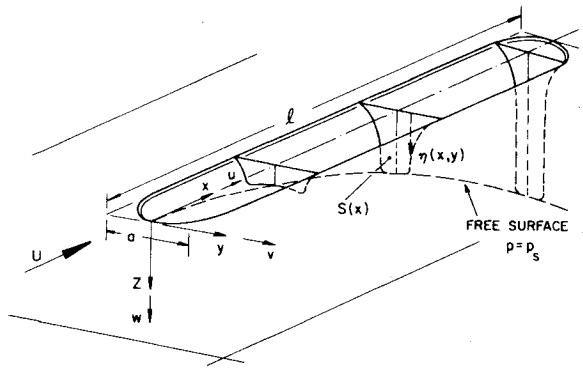

Fig. 1 Flow through a slot.

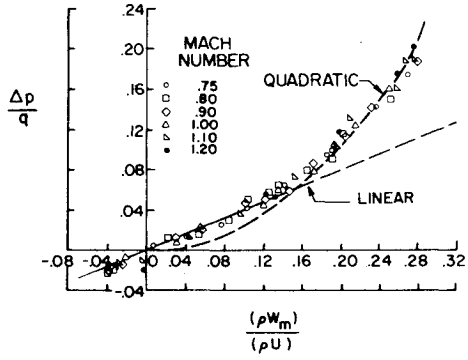

Fig. 2 Experimentally determined characteristics of a single slender slot[1] [note: linear curve chosen to best fit data; quadratic curve computed from Eq. (62)].

body theory is that forces arise from regions in which the cross flow experiences a streamwise rate of change, i.e., only from regions of the body where the cross-sectional area, shape, or incidence angle is changing. Linear behavior can also be derived from the local averaged boundary condition for a row of slots by integration in the streamwise direction. The effect arises from the streamline curvature term which represents the convective acceleration of the cross flow (any linear terms that may be present will also contribute).

Taking another point of view sometimes used in connection with slender body theory,[7] suppose the cross flow is observed in a plane being convected with the freestream. The cross flow will then appear as a two-dimensional unsteady flow through a slit. As soon as the plane is convected past the slot leading edge the cross flow will begin to accelerate. Fundamentally, it is this cross flow acceleration which causes the linear behavior, and it is present even when the free surface displacement in the slot is small. Once the free surface displacement becomes significant, the effective mass of fluid that participates in the cross flow acceleration will begin to increase since the amount of fluid that has receded into the slot will also become important. Finally, when the free surface displacement becomes large compared to the slot width, the cross flow will resemble a fully developed orifice or jet flow in which the pressure differential will depend primarily on the square of the normal velocity.

In addition to the effects just mentioned, the analysis also shows that in the linear regime the magnitude of the cross flow at any point along the slot is affected significantly by the magnitude of the cross flow at other points along the slot. However, the influence of other points along the slot is found to be higher order in the quadratic regime. These results are a direct consequence of the formal application of slender-body theory to this problem. The interaction between points along the slot appears in the analysis through terms in the outer solution involving the sink strength distribution in the streamwise direction.

Formulation

Assume that the fluid is steady and irrotational, then the governing equation is

$$\nabla^2\Phi - \frac{1}{c^2}u\cdot\nabla\left(\frac{u^2}{2}\right)=0 \tag{1}$$

where $\Phi(x,y,z)$ is the velocity potential such that the velocity vector is given by

$$u=\nabla\Phi \tag{2}$$

The configuration of the slot and the coordinate system are as shown in Fig. 1. The slot is assumed to lie in an infinite plane below a uniform freestream. In particular, the case of a nonuniform external flowfield is not considered and the important case of transonic flow is also excluded.

The problem will be formulated in terms of the method of matched asymptotic expansions and some aspects of the development are similar to the treatment of slender body theory in Ref. 7. The variables can be scaled in different ways depending on which slot cross flow regime is of interest. However, in the development that follows, a method of scaling is used which is valid in general. The limiting cases of small and large free surface displacements, corresponding to linear and quadratic behavior, then can be extracted easily for detailed analysis. The relationship between this general scaling method and other methods will be mentioned at the appropriate points.

The velocity potential can be expressed as

$$\Phi=Ux+a\sqrt{2\Delta p/\rho}\,\phi \tag{3}$$

where ϕ is a nondimensional perturbation velocity potential. Here $\Delta p=p_\infty-p_s$ is the difference between the freestream static pressure and the pressure at the free surface in the slot. When there is no static pressure difference across the plane containing the slot, i.e., $\Delta p=0$, then the effect of the slot vanishes. The inner length scale is defined to be the maximum slot width a. The relevant small parameter for the problem is

$$\epsilon=\sqrt{\Delta p/q} \tag{4}$$

where $q=\frac{1}{2}\rho U^2$. This parameter is a measure of the flow deflection angle in the slot. Then the outer length scale is defined to be $L=a/\epsilon$. Notice that the slot length ℓ is not chosen to be the outer length scale, since it is not necessarily the appropriate scale for variations in the streamwise direction. The length L measures the streamwise distance over which the free surface deflection becomes comparable to the slot width, and is thus the appropriate length scale for the development of the slot cross flow.

The following nondimensionalization is used for the variables:

$$\Phi=LU_\infty\Phi^* \quad u=U_\infty u^* \quad x=Lx^*, \quad y=Ly^*, \quad z=Lz^* \tag{5}$$

where the notation $(\,)^*$ indicates a nondimensional quality. This leads to a nondimensional outer expansion of the form

$$\Phi^*=x^*+\epsilon^2\phi^*(x^*,y^*,z^*)+\ldots \tag{6}$$

In nondimensional form Eq. (1) becomes

$$\nabla^{*2}\Phi^*-M^2u^*\cdot\nabla^*(u^{*2}/2)=0 \tag{7}$$

where $M=U/c$ is the Mach number. Substituting the outer expansion Eq. (6) into Eq. (7) and retaining terms that are $0[\epsilon^2]$ gives

$$(1-M^2)\frac{\partial^2\phi^*}{\partial x^{*2}}+\frac{\partial^2\phi^*}{\partial y^{*2}}+\frac{\partial^2\phi^*}{\partial z^{*2}}=0 \tag{8}$$

The inner variables are defined by a stretching of the cross flow coordinates

$$\bar{y}=y^*/\epsilon, \qquad \bar{z}=z^*/\epsilon \tag{9}$$

(note that $\bar{y}=y/a$ and $\bar{z}=z/a$). Then assume an inner expansion of the form

$$\bar{\Phi}=x^*+\epsilon^2\bar{\phi}(x^*,\bar{y},\bar{z}) \tag{10}$$

Substituting into either Eq. (7) or (8) gives, to lowest order,

$$\frac{\partial^2\bar{\phi}}{\partial\bar{y}^2}+\frac{\partial^2\bar{\phi}}{\partial\bar{z}^2}=0 \tag{11}$$

which shows that the inner region behaves as a two-dimensional potential flow in the cross flow plane.

For convenience, the notation ( )* is now dropped with the understanding that unmarked variables are still nondimensionalized according to Eq. (5), unless otherwise indicated.

The boundary conditions for the problem are that

$$\nabla\phi\to 0 \text{ as } \sqrt{x^2+y^2+z^2}\to\infty, \quad \partial\phi/\partial z|_{z=0}=0 \text{ on the rigid wall} \tag{12}$$

$p=\text{const}=p_s$ on the free surface in the slot, and free surface slope = 0 at the slot leading edge. The first and second of these conditions are applied to the outer velocity potential $\phi(x,y,z)$, whereas the second, third, and fourth conditions are applied to the inner velocity potential $\bar{\phi}(x,\bar{y},\bar{z})$. Any indeterminancy that remains after the application of the appropriate boundary conditions to each solution is resolved when the solutions are matched. For the outer solution, to the present order of expansion, the slot appears as a line of sinks distributed along the x axis. The strength of this distribution is determined by matching with the inner solution, as is usual with slender body theory.

The boundary conditions for the inner solution require close examination. The equation for pressure in dimensional form is

$$\frac{p-p_\infty}{q}=\frac{2}{\gamma M^2}\left\{\left[1-\frac{\gamma-1}{c^2}\left(\frac{|\nabla\Phi|^2-U^2}{2}\right)\right]^{\gamma/(\gamma-1)}-1\right\} \tag{13}$$

After re-expressing in inner variables, setting $p=p_s$, retaining only the lowest order terms, and again dispensing with the ( )* notation, this equation becomes

$$\left[2\frac{\partial\bar{\phi}}{\partial x}+\left(\frac{\partial\bar{\phi}}{\partial\bar{y}}\right)^2+\left(\frac{\partial\bar{\phi}}{\partial\bar{z}}\right)^2\right]\Bigg|_{\text{fs}}=1 \tag{14}$$

The notation fs means the equation applies only on the free surface. This is the condition that the free surface be at constant pressure.

The unknown position of the free surface expressed in inner variables is

$$\bar{z}=\bar{\eta}(x,\bar{y}), \qquad \text{for } |\bar{y}|\le t(x) \tag{15}$$

where $t(x)$ is the slot thickness distribution function chosen so that the (dimensional) slot thickness is $a\cdot t(x)$. The solution must satisfy the condition that the flow be tangent to the free surface at the free-surface location. If the free surface is described by

$$B(x,y,z)=\bar{B}(x,\bar{y},\bar{z})=\bar{z}-\bar{\eta}(x,\bar{y})=0 \tag{16}$$

then in dimensional coordinates the flow tangency condition is

$$\nabla B\cdot u=\nabla B\cdot\nabla\Phi=0 \tag{17}$$

After re-expressing in nondimensional variables, retaining only the lowest order terms, and using Eq. (16), the flow tangency condition in inner variables becomes

$$\left[\frac{\partial\bar{\eta}}{\partial x}+\frac{\partial\bar{\eta}}{\partial\bar{y}}\frac{\partial\bar{\phi}}{\partial\bar{y}}-\frac{\partial\bar{\phi}}{\partial\bar{z}}\right]\Bigg|_{\text{fs}}=0 \tag{18}$$

Solutions and Matching

The general free surface problem in the slot would be extremely difficult to solve. Therefore, this section is restricted to general comments on the solution structure and on the matching procedure.

Referring to Eq. (11) the inner solution must have the form

$$\bar{\phi}=\bar{\phi}_c(x,\bar{y},\bar{z})+g(x) \tag{19}$$

As is usual for slender body theory, far from the slot the velocity potential $\bar{\phi}_c(x,\bar{y},\bar{z})$ will look like a simple source or sink whose strength is related to the rate of change of the cross-sectional area, $\bar{S}(x)$, occupied by the flow in the slot. Thus

$$\bar{\phi}\simeq-[\bar{S}'(x)/\pi]\ell n\bar{r}+g(x)\equiv\bar{\phi}^o \text{ as } \bar{r}\to\infty \tag{20}$$

where $\bar{r}=\sqrt{\bar{y}^2+\bar{z}^2}$ and $\bar{\phi}^o$ is the outer limit of the inner solution. In dimensional form, the cross-sectional area is $S=a^2\bar{S}$.

The outer solution can be expressed as an integral over a line of sinks distributed along the slot length. For subsonic flow

$$\phi=\frac{1}{2\pi}\int_0^{\ell^*}\frac{f(x_1)\,dx_1}{\sqrt{(x-x_1)^2+r^2}} \tag{21}$$

where $\ell^*=\ell/L$ is the nondimensional slot length and $r=\sqrt{y^2+z^2}$. This integral can be shown to have the following form when r is small[7]:

$$\phi=-\frac{f(x)}{\pi}\ell nr-\frac{f(x)}{2\pi}\ell n\frac{\beta^2}{4x(\ell^*-x)}+\frac{1}{2\pi}\int_0^{\ell^*}\frac{f(x_1)-f(x)}{|x-x_1|}dx_1 \tag{22}$$

where $\beta^2\equiv 1-M^2$. Re-expressing this outer solution for small r in inner variables gives the inner limit of the outer solution

$$\phi^i=-\frac{f(x)}{\pi}\ell n\bar{r}-\frac{f(x)}{2\pi}\ell n\frac{\epsilon^2\beta^2}{4x(\ell^*-x)}+\frac{1}{2\pi}\int_0^{\ell^*}\frac{f(x_1)-f(x)}{|x-x_1|}dx_1 \tag{23}$$

Here $\ell n\,\epsilon$ is treated as an order one quantity, as is often done in slender-body theory. Alternatively, this problem could be treated more formally by a modification of the expansion procedure, but the results would be the same.

The matching procedure requires that the inner limit of the outer solution equal the outer limit of the inner solution: $\phi^i=\bar{\phi}^o$. Using Eqs. (20) and (23), the matching shows that

$$\bar{S}'(x)=f(x) \tag{24}$$

and then

$$g(x)=-\frac{\bar{S}'(x)}{2\pi}\ell n\frac{\epsilon^2\beta^2}{4x(\ell^*-x)}+\frac{1}{2\pi}\int_0^{\ell^*}\frac{\bar{S}'(x_1)-\bar{S}'(x)}{|x-x_1|}dx_1 \tag{25}$$

Equation (25) applies only for subsonic flow. A similar development for supersonic flow[7] leads again to Eq. (24) and a different expression for $g(x)$

$$g(x) = -\frac{\bar{S}'(x)}{\pi}\ell n\frac{\epsilon B}{2x} + \frac{1}{\pi}\int_0^x \frac{\bar{S}'(x_1)-\bar{S}'(x)}{|x-x_1|}dx_1 \qquad (26)$$

where $B^2 = M^2 - 1$.

Now the problem for flow in the inner region can be restated. The velocity potential is given by Eq. (19) with

$$\frac{\partial^2\bar{\phi}_c}{\partial\bar{y}^2} + \frac{\partial^2\bar{\phi}_c}{\partial\bar{z}^2} = 0 \qquad (27)$$

Far from the slot

$$\bar{\phi}_c - \frac{-\bar{S}'(x)}{\pi}\ell n\bar{r} \to 0 \text{ as } \bar{r}\to\infty \qquad (28)$$

In the slot the constant pressure boundary condition Eq. (14) becomes

$$\left[2\frac{\partial\bar{\phi}_c}{\partial x} + \left(\frac{\partial\bar{\phi}_c}{\partial\bar{y}}\right)^2 + \left(\frac{\partial\bar{\phi}_c}{\partial\bar{z}}\right)^2\right]\Big|_{fs} = 1 - 2g'(x) \qquad (29)$$

where $g(x)$ is given by Eq. (25) or (26), depending on whether the flow is subsonic or supersonic, respectively. The flow tangency condition Eq. (18) is

$$\left[\frac{\partial\bar{\eta}}{\partial x} + \frac{\partial\bar{\eta}}{\partial\bar{y}}\frac{\partial\bar{\phi}_c}{\partial\bar{y}} - \frac{\partial\bar{\phi}_c}{\partial\bar{z}}\right]\Big|_{fs} = 0 \qquad (30)$$

These equations constitute the final form of the inner problem. The difficulty in solving the problem as posed is that both the free surface displacement η and the velocity potential are unknown. Certain limiting cases are solved next.

Slot Flow for Small Free Surface Displacements

The nondimensional slot length is $\ell^* = \ell/L = \epsilon\ell/a$. When $\epsilon \ll a/\ell$ then $x \le \ell^* \ll 1$. Under these conditions, since ϵ measures the flow deflection angle in the slot, the free surface displacement is very small compared to the slot width and the pressure boundary condition can be applied on $\bar{z}=0$. Furthermore, in this case the quadratic terms in the pressure boundary condition Eq. (29) can be neglected. Let $\Phi = UL\bar{\Phi} = U\ell\hat{\Phi}$ and $x = Lx^* = \ell\hat{x}$. Introducing the new nondimensional variables $\hat{\Phi}$ and $\hat{x}$ into Eq. (14) or (29) shows that the quadratic terms are smaller than the other terms by a factor ℓ^{*2}. A similar result can be obtained by redefining the velocity potential as $\hat{\Phi} = \hat{x} + \epsilon^2\hat{\Phi}$ and solving the problem from the beginning with outer length ℓ and inner length a. This approach, which is in fact a more traditional scaling for slender body theory, is satisfactory for the present case of small free surface displacement. However, since it excludes the quadratic terms in the pressure boundary condition, it is not a completely general approach.

With the quadratic terms neglected, the pressure boundary condition becomes

$$\frac{\partial\bar{\phi}_c}{\partial x}\Big|_{z=0} = \tfrac{1}{2} - g'(x), \qquad |y| \le \tfrac{1}{2}t(x) \qquad (31)$$

The following function will satisfy this simplified pressure boundary condition

$$\bar{\phi}_c(x,\bar{y},\bar{z}) = \left(\frac{x}{2} - g(x) + C_1\right)\phi_1(x,\bar{y},\bar{z}) \qquad (32)$$

where C_1 is an arbitrary constant. The potential ϕ_1 must be a solution of the two-dimensional Laplace equation in the cross flow plane and must satisfy the boundary conditions

$$\frac{\partial\phi_1}{\partial\bar{z}}\Big|_{\bar{z}=0} = 0, \qquad |\bar{y}| > \tfrac{1}{2}t(x) \qquad (33)$$

$$\phi_1|_{\bar{z}=0} = 1, \qquad |\bar{y}| < \tfrac{1}{2}t(x) \qquad (34)$$

In addition, ϕ_1 must behave such that ϕ_c satisfies the far field condition imposed by Eq. (28).

The flow rate into the slot at any streamwise location equals the rate of change of cross-sectional area, therefore,

$$\bar{S}'(x) = \int_{-t(x)/2}^{t(x)/2}\frac{\partial\bar{\phi}_c}{\partial\bar{z}}\Big|_{\bar{z}=0}d\bar{y} = \left(\frac{x}{2} - g(x) + C_1\right)\bar{w}t(x) \qquad (35)$$

where

$$\bar{w} \equiv \frac{1}{t(x)}\int_{-t(x)/2}^{t(x)/2}\frac{\partial\bar{\phi}_1}{\partial\bar{z}}\Big|_{\bar{z}=0}d\bar{y} \qquad (36)$$

The quantity $\bar{w}$ is the average velocity entering the slot at a given streamwise location.

The real valued velocity potential which satisfies the conditions stated earlier is

$$\phi_1(x,\bar{y},\bar{z}) = \mathrm{Re}\left\{1 - \frac{1}{\ell n4}\ell n[2\tilde{\zeta} + \sqrt{1+(2\tilde{\zeta})^2}]\right\} \qquad (37)$$

where $\tilde{\zeta} = (\bar{z} + i\bar{y})/t(x)$ is a complex variable. This velocity potential is associated with the potential flow through a slit. The velocity field exhibits a square-root singularity at the side edges $\bar{y} = \pm\tfrac{1}{2}t(x)$. A brief calculation gives

$$\bar{w} = \frac{\pi}{\ell n4} \qquad (38)$$

Returning to Eq. (39) and substituting for $g(x)$ from Eq. (27) for subsonic flow yields an integral equation for $\bar{S}'(x)$

$$\frac{1}{\bar{w}t(x)}\bar{S}'(x) = \frac{x}{2} + C_1 + \frac{\bar{S}'(x)}{2\pi}\ell n\frac{\epsilon^2\beta^2}{4x(x-x_1)} - \frac{1}{2}\int_0^{\ell^*}\frac{\bar{S}'(x_1)-\bar{S}'(x)}{|x-x_1|}dx_1 \qquad (39)$$

The presence of the arbitrary constant C_1 allows the application of a flow tangency condition at the front of the slot, namely $\bar{S}'(0) = 0$. Assuming that $\bar{S}'(x)$ goes to zero sufficiently fast as $x\to 0$,

$$C_1 = \int_0^{\ell^*}\frac{\bar{S}'(x_1)}{x_1}dx_1 \qquad (40)$$

Now that the equation has been formulated, it is convenient to change to a new dimensionless variable $\hat{x}$ such that

$$x^* = \epsilon(\ell/a)\hat{x} \qquad (41)$$

(In dimensional variables $\hat{x} = x/\ell$.) Again dropping the ( )* notation, it follows that

$$\bar{S}'(x) = \bar{S}'(\hat{x})/(\epsilon\ell/a) \qquad (42)$$

Then, using Eqs. (42-46) the integral equation for subsonic flow becomes

$$\bar{S}'(\hat{x})\left\{\ell n\left[\frac{(\ell/a)^2}{1-M^2}\right] + \ell n[4\hat{x}(1-\hat{x})] + \frac{\ell n16}{t(\hat{x})}\right\} = \pi\left(\epsilon\frac{\ell}{a}\right)^2\hat{x} + \int_0^1\frac{\bar{S}'(\xi)}{\xi}d\xi + \int_0^1\frac{\bar{S}'(\hat{x})-\bar{S}'(\xi)}{|\hat{x}-\xi|}d\xi \qquad (43)$$

Repeating the derivation for the case of supersonic flow gives

$$\bar{S}'(\hat{x})\left\{\ell n\left[\frac{(\ell/a)^2}{M^2-1}\right]+\ell n[4\hat{x}^2]+\frac{\ell n 16}{t(\hat{x})}\right\}$$
$$=\pi\left(\epsilon\frac{\ell}{a}\right)^2\hat{x}+2\int_0^{\hat{x}}\frac{\bar{S}'(\hat{x})-\bar{S}'(\xi)}{|\hat{x}-\xi|}\,d\xi \tag{44}$$

Now $C_1=0$ to give $\bar{S}'(0)=0$, the consistent end condition for slender-body theory.

Clearly, from the form of these integral equations, the solutions must have the form

$$\bar{S}(\hat{x})=\left(\epsilon\frac{\ell}{a}\right)^2 F\left(\hat{x},\ell n\frac{\ell/a}{|1-M^2|}\right) \tag{45}$$

The function F depends on the assumed slot geometry, namely, on the particular choice of $t(\hat{x})$. Recalling the dimensional relationships $\hat{x}=1$ for $x=\ell$ and $a^2\bar{S}(\hat{x})=S(x)$, where x is now a dimensional variable, gives

$$S(\ell)=\epsilon^2\ell^2 F\left(1,\ \ell n\frac{\ell/a}{|1-M^2|}\right)\equiv\frac{\epsilon^2\ell^2}{G\left(\ell n\dfrac{\ell/a}{|1-M^2|}\right)} \tag{46}$$

The function G is defined by the above expression.

The flow rate from the slot is, to lowest order,

$$Q=U\cdot S(\ell)=w_m a\ell A_f \tag{47}$$

where w_m is the mean normal velocity averaged over the entire slot and the area factor is defined as

$$A_f=\int_0^1 t(\hat{x})\,d\hat{x} \tag{48}$$

Combining Eqs. (46), (47), and (4) gives the result

$$\frac{\Delta p}{q}=\frac{a}{\ell}A_f G\frac{w_m}{U} \tag{49}$$

This equation shows a linear relationship between the pressure difference across the slot and the mean normal velocity through the slot. Recall that Eq. (49) holds only for $\epsilon\ll a/\ell$, i.e., only for small free surface displacement. This is consistent with the fact that linear behavior is observed experimentally when the flow rate through the slot is small.

Note that the linear relationship just derived holds even for an untapered slot, namely $t(\hat{x})=1$ for $0<\hat{x}<1$. The problem in this case is that slender-body theory is not valid near the leading and trailing edges of an untapered slot. However, there is no reason to believe that the conclusion about linear behavior is affected since there will still be a rate of change of the cross-sectional area as the cross flow develops downstream of the leading edge. The difficulty near the leading and trailing edges of an untapered slot could be removed by including local three-dimensional solutions in these regions.

The slope of the pressure difference vs velocity curve is $(a/\ell)A_f G$. The quantity a/ℓ is roughly the aspect ratio of the slot. Its appearance is analogous to the familiar result in slender wing theory that the lift curve slope is proportional to the aspect ratio. The fact that the argument of the function G is logarithmic suggests that its dependence on slot aspect ratio and Mach number is relatively weak. An integral equation must be solved for a specified slot taper $t(\hat{x})$ to determine the function G. That integral equations arise in this problem is related to the fact that the flow rate at any point along the slot affects the pressure, and thus the flow rate, at other locations along the slot.

Analytical Solutions for Small Free Surface Displacement

An examination of Eqs. (43) and (44) for subsonic and supersonic slot flows shows that in each case a particular choice of the slot taper, $t(\hat{x})$, allows a simple analytical solution to be found. Fortunately, the required slot taper functions give rise to fairly realistic slot planforms. In both cases $t(\hat{x})$ is chosen to remove the logarithmic dependence on $\hat{x}$ appearing on the left-hand sides of Eqs. (43) and (44).

$$t(\hat{x})_{\text{subsonic}}=\ell n 16\Big/\ell n\left[\frac{4}{\hat{x}(1-\hat{x})}\right] \tag{50}$$

and

$$t(\hat{x})_{\text{supersonic}}=\ell n 16\Big/\ell n\left[\frac{16}{\hat{x}^2}\right] \tag{51}$$

The corresponding slot planforms are shown in Fig. 3.

Direct substitution shows that the solution in both cases is simply

$$\bar{S}'(\hat{x})=\left(\epsilon\frac{\ell}{a}\right)^2\frac{\pi}{2}\hat{x}\Big/\left\{\ell n\left[\frac{4\ell/a}{\sqrt{|1-M^2|}}\right]-1\right\} \tag{52}$$

Integrating and using Eq. (50) gives

$$G=\frac{4}{\pi}\left\{\ell n\left[\frac{4\ell/a}{\sqrt{|1-M^2|}}\right]-1\right\} \tag{53}$$

Direct integration of $t(x)$ using Eq. (48) gives the area factors

$$A_{f_{\text{subsonic}}}=0.848,\quad A_{f_{\text{supersonic}}}=0.677 \tag{54}$$

All the information required by Eq. (49) to relate pressure difference to the mean normal velocity through slot is now available. As an example, suppose $\ell/a=10$. Then for subsonic flow $A_f G=0.29$ for $M=0$ and $A_f G=0.38$ for $M=0.9$; for supersonic flow $A_f G=0.27$ for $M=1.2$. Note, however, that the slot shapes in subsonic and supersonic flow are different. These results are certainly in qualitative agreement in both magnitude and trend with available experimental data.[1,8] A more detailed comparison with experiment is made in the next section.

Numerical Calculations

Numerical solutions were obtained for various slot taper distributions using the method described in the Appendix. The

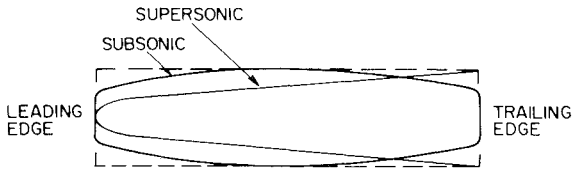

Fig. 3 Slot planform shapes for which an analytical solution can be found.

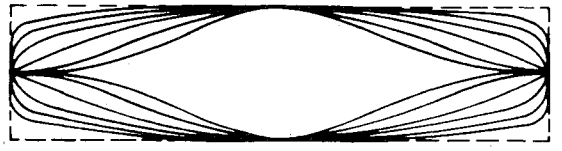

Fig. 4 Slot planform shapes for the family $t(x)=[4x(1-x)]^{\sigma_n}$ where $\sigma_n=4, 2, 1, \frac{1}{2}, \frac{1}{4}, \frac{1}{8}$ (from pointed to blunt).

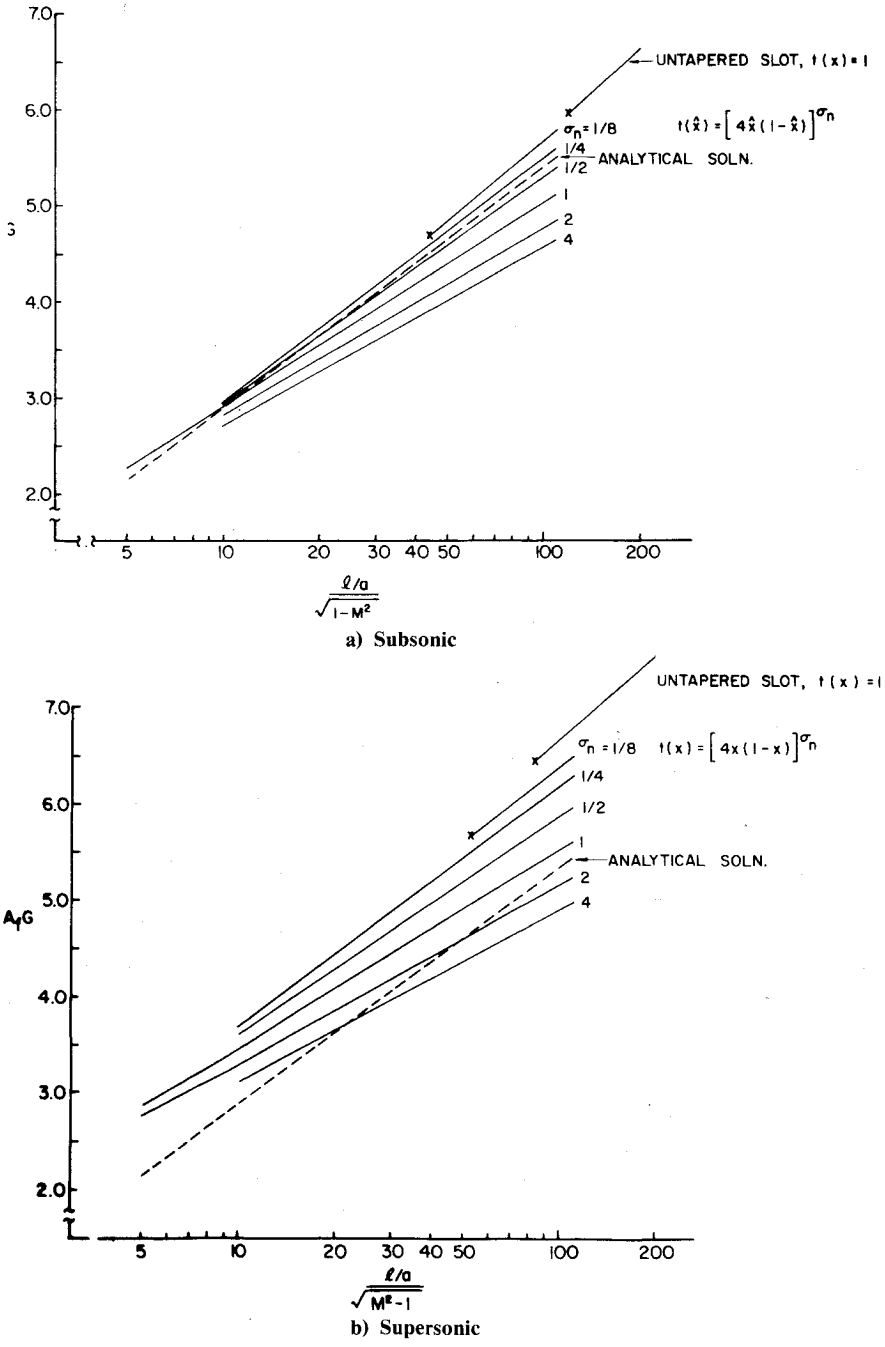

Fig. 5 Numerical solutions for the proportionality constant A_fG; the notation × — indicates the last value for which the numerical method converged.

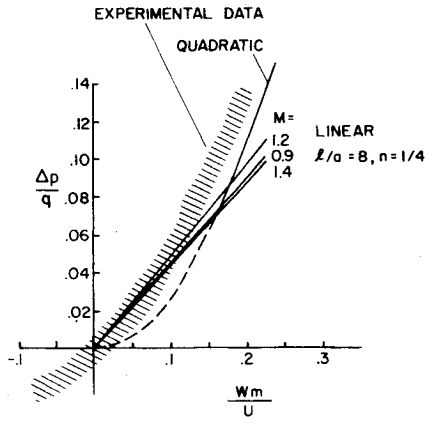

Fig. 6 Comparison between theory and experiment (data from Ref. 8); experimental Mach numbers equal 0.9, 1.0, 1.2, 1.3, 1.4 for a slot having $\ell/a = 8$.

effort was concentrated primarily on the family of taper functions

$$t(\hat{x}) = [4\hat{x}(1-\hat{x})]^{\sigma_n} \tag{55}$$

where $\sigma_n = 1, 2, 4$ for sharp pointed slots, and $\sigma_n = \frac{1}{2}, \frac{1}{4}, \frac{1}{8}$ for blunt slots. This family of slot planforms is shown in Fig. 4.

For each slot the product A_fG, which appears in Eq. (49), was calculated as a function of $(\ell/a)\,|1-M^2|^{-\frac{1}{2}}$ for both subsonic and supersonic flow, see Figs. 5a and 5b. The analytical solutions described previously are also presented for comparison. The variation of A_fG with σ_n is remarkably small considering the substantial change in the corresponding slot planform shape. This indicates that taper alone is not responsible for the linear behavior predicted for the pressure difference vs mean slot velocity curve. In addition, the quantity A_fG increases as the slot becomes more blunt. This trend also supports the assertion that the linear behavior will still be present for an untapered slot.

Because of convergence problems with the iterative method used to obtain numerical solutions, results for an untapered slot ($\sigma_n \to 0$) and for other very blunt slots could only be obtained for large values of the parameter $\ell/a\,|1-M^2|^{-1/2}$. It was found that as the slot becomes more blunt, the method requires an increasingly accurate initial guess in order to converge. The actual solution obtained was always independent of the initial guess, as should be the case. The convergence problem is probably related to the failure of slender-body theory near ends of a blunt slot.

To illustrate the type of results obtained, Fig. 6 shows calculations of pressure difference vs mean slot flow for a fairly blunt slot ($n = 1/4$) having $\ell/a = 8$ for different values of Mach number. As stated in their derivation, the linear curves apply to the case of small flow deflection in the slot. The quadratic curve also shown in Fig. 6 approximates the behavior for very large flow deflections in an untapered slot. This curve is derived in the next section. In the intermediate region where the linear and quadratic curves intersect, neither of these limiting cases applies.

The cross-hatched region shows the range of experimental data for an untapered slot with $\ell/a = 8$ measured at the same Mach numbers.[8] The data showed no consistent Mach number dependence; apparently it is obscured by experimental scatter. The measurements were made using a plate of 10% porosity with many small slots ($1/2 \times 1/16$ in.). Actually, the data is not well-suited for quantitative comparison with the theory because the slots, due to their small size, may have been under a relatively thick boundary layer and because the plate in which the slots were cut had a thickness that was equal to the slot width. Also, the present theory does not account for interference between slots. Viewed in this light, the agreement between theory and experiment is most encouraging. There is, however, a definite need for an appropriate set of experimental data for comparison with the theoretical results. Unfortunately the cleaner data presented in Ref. 1 and shown in Fig. 2 cannot be used for comparison since the ratio ℓ/a for that slot was not given.

Finally, it is worth noting that since slender body theory works reasonably well for lifting surfaces of aspect ratio less than approximately one half,[7] the present results should be applicable to holes in this same aspect ratio range, as well as for very slender slots. Thus, this work may be of some use in predicting the behavior of holes in perforated wind tunnel walls.

Fully Developed Flow through the Slot

When $a/\ell \ll \epsilon \ll 1$ the cross flow in the slot will resemble closely a fully developed jet or orifice flow (depending on the slot cross-sectional geometry) over most of the slot length. One purpose of this section is to show that the general formulation of the problem presented earlier is also consistent with this case. In this limit $\ell^* = \ell/L = \epsilon\ell/a \gg 1$, so $L \ll \ell$. Since L is the length scale over which the free surface deflection is comparable to the slot width, the cross flow becomes fully developed near the slot leading edge. The general formulation outlined earlier is required to analyze the cross-flow development. However, the average behavior of the slot will be dominated by the region of fully developed cross flow which encompasses most of the slot length. For this reason only the fully developed cross-flow region will be considered.

The length scale for variations in the fully developed cross flow is ℓ, since these variations can only come from slot taper or from the influence of points at other streamwise stations [the $g'(x)$ term in Eq. (29)]. Since the length scale L is used in the general formulation, x should be renormalized. Again introduce the variable $\hat{x}$ such that $x = Lx^* = \ell\hat{x}$, from which $x = \hat{x}^*/\ell^*$. This variable change can be accomplished by applying the chain rule to the x derivatives in Eq. (29)

$$\frac{\partial\tilde{\phi}_c}{\partial x^*} = \frac{1}{\ell^*}\frac{\partial\tilde{\phi}_c}{\partial\hat{x}} \quad \text{and} \quad g'(x^*) = \frac{1}{\ell^*}g'(\hat{x}) \tag{56}$$

Since $\ell^* \gg 1$, these derivative terms can be neglected in Eq. (29). An error of the same size is incurred by ignoring the portion of the slot in which the cross flow is developing. Therefore, the pressure boundary condition for most of the slot becomes

$$\left[\left(\frac{\partial\tilde{\phi}}{\partial\tilde{y}}\right)^2 + \left(\frac{\partial\tilde{\phi}}{\partial\tilde{z}}\right)^2\right]\Bigg|_{fs} = 1 \tag{57}$$

The same result applies for both subsonic and supersonic flow. The strength of the fully developed cross flow is therefore determined locally and controlled by the nonlinear terms in the pressure boundary condition.

Thus, to good approximation, the velocity potential for the equivalent steady two-dimensional free surface flow can be used, provided the changes in free surface shape are confined to the region where the flow has become essentially parallel and the pressure is nearly constant ($=p_s$). This situation is illustrated in Fig. 7 for the case of a sharp edged slot.

To obtain the relationship between pressure difference and flow through an untapered slot it is not necessary to consider the velocity potential in any detail. Suppose that the final width of the jet leaving a slot is a fraction σ of the local slot width. The precise value of σ depends on the slot geometry, where $\sigma = 0.611$ for a sharp edged slot, and $\sigma = 1.0$ for a thick slot without internal flow separation. Applying the boundary condition to the cross flow in the region downstream of the slot where the flow is almost parallel gives

$$\tilde{w}_f^2 = 1 \tag{58}$$

where $\tilde{w}_f$ is the final cross flow velocity beneath the slot. Then,

$$\tilde{S}'(x) = \sigma t(x)\,\tilde{w}_f = \sigma t(x) \tag{59}$$

Integrating once yields

$$\tilde{S}(x) = \sigma\int_0^x t(x)\,dx \tag{60}$$

A constant of integration that could be added to Eq. (59) has been omitted since the region near the leading edge is being neglected. Setting $x = \ell^*$ and re-expressing in dimensional form gives

$$S(\ell) = \epsilon\sigma a\ell A_f \tag{61}$$

where A_f was defined in Eq. (48). As before, the flow rate through the slot is defined by Eq. (47). Hence, combining Eqs. (61), (47), and (4) gives the result

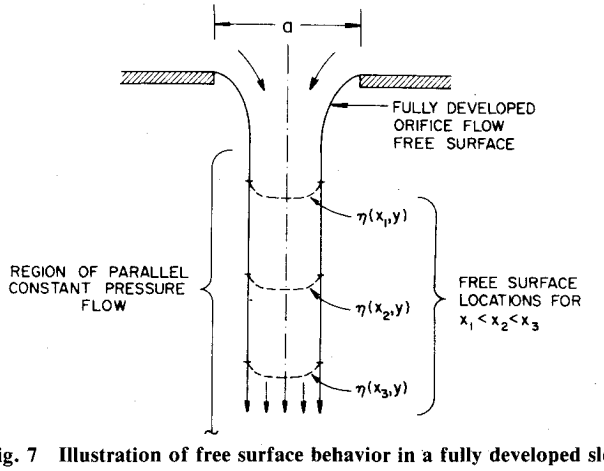

Fig. 7 Illustration of free surface behavior in a fully developed slot cross flow.

$$\frac{\Delta p}{q} = \frac{1}{\sigma^2}\left(\frac{w_m}{U}\right)^2 \tag{62}$$

This equation was used to generate the quadratic behavior curve in Figs. 2 and 6 assuming a sharp edged slot; note that the agreement with the data is good, especially in Fig. 2.

Concluding Remarks

The analysis has shown that the experimentally observed aerodynamic behavior of a wind tunnel wall slot can be predicted using inviscid slender-body theory. Only the simplest problem of a single isolated slot has been studied. Nevertheless, the important conclusion can be drawn that there is a theoretical basis for a linear relationship between pressure difference and normal velocity through the slot. This relationship has been analyzed for the case when the normal velocity is sufficiently small that the free surface deflection is small compared to the slot width. Fundamentally, the linear behavior occurs as a result of the convective acceleration of the cross flow into the slot. The mutual aerodynamic interaction of points along the slot must be taken into account in order to predict the overall slot behavior. At high flow rates through the slot the behavior is dominated by the nonlinear terms in the cross flow, and all other effects are higher order. In this limit the overall behavior of the slot is governed by a simple formula.

Appendix: Numerical Methods

The numerical solutions of the integral Eqs. (43) and (44) presented in this paper were obtained through an iterative procedure. A second procedure in which the integral equation was replaced by a set of linear algebraic equations was used to check the iterative procedure in a few cases. However, in terms of the number of subdivisions of the slot interval required to obtain an accurate answer, the iterative method proved to be vastly superior.

As the slot planform became more blunt, the iterative method would not converge unless the initial guess for the solution was close to the final answer. This problem could usually be overcome by starting with a slot planform for which the solution was known and moving in increments toward the desired solution while updating the initial guess at each step. Convergence was often obtained within a few iterations, but as the slots became more blunt more iterations were required. The convergence was generally more rapid when the parameter $\ell/a\,|1-M^2|^{-1/2}$ was large. The method did not converge for very blunt slots or for a rectangular slot unless the value of this parameter was quite large. The iteration procedure was terminated when the solution value at every point was within 1% of the corresponding value in the preceding iteration.

As a convenience define a function $y(\hat{x})$ such that

$$\bar{S}'(\hat{x}) = \pi(\epsilon\ell/a)^2 y(\hat{x}) \tag{A1}$$

For subsonic flow, the form of Eq. (43) used to find the solution by iteration is

$$y^{(m+1)}(\hat{x}_i) = \left[\ell n\left\{\frac{(2\ell/a)^2}{1-M^2}\hat{x}_i(1-\hat{x}_i)\right\} + \frac{\ell n 16}{t(\hat{x}_i)}\right]^{-1} \times\left\{\hat{x}_i + \Delta\xi\sum_{j=1}^{n}\frac{y^{(m)}(\xi_j)}{\xi_j} + \Delta\xi\sum_{j=1}^{n}\frac{y^{(m)}(\hat{x}_i)-y^{(m)}(\xi_j)}{|\hat{x}_i-\xi_j|}\right\} \tag{A2}$$

where

$$y(\xi_j) = \tfrac{1}{2}y^{(m)}(\hat{x}_i) \quad \text{for } j=1$$

$$y(\xi_j) = \tfrac{1}{2}[y^{(m)}(\hat{x}_j) + y^{(m)}(\hat{x}_{j-1})] \quad \text{for } j=2,\ldots,n \tag{A3}$$

The n values of $\hat{x}_i$ were determined by dividing the interval from $0\le x\le 0.999$ into n equal increments, so that $\hat{x}_1 = 0.999/n$, etc. The n values of ξ_j were determined by placing these points halfway between the $\hat{x}_i$ stations, giving $\xi_1 = \tfrac{1}{2}0.999/n$, etc. Values of n between 20 and 100 were used; the larger values were required to obtain adequate resolution near the leading and trailing edges of relatively blunt slot planforms. Tests showed that the converged solution did not depend on the number of increments in the interval, provided of course that a sufficiently large number was chosen.

The form of Eq. (44) used for finding the numerical solution in supersonic flow is

$$y_i^{(m+1)}(\hat{x}) = \left[\ell n\left\{\frac{(2\ell/a)^2}{M^2-1}\hat{x}_i^2\right\} + \frac{\ell n 16}{t(\hat{x}_i)}\right]^{-1} \times\left\{\hat{x}_i + 2\Delta\xi\sum_{j=1}^{i}\frac{y(\hat{x}_i)-y(\xi_j)}{|\hat{x}_i-\xi_j|}\right\} \tag{A4}$$

Some typical solution curves for $y(\hat{x})$ [proportional to $\bar{S}'(\hat{x})$] are shown in Figs. A1a and A1b for the slot planform family of Eq. (55). When the ends are cusped ($\sigma_n > 1$) the slope of $y(\hat{x})$ is zero at both ends and its maximum value occurs near the center of the slot. As the ends of the slot become blunt ($\sigma_n < 1$) the maximum value moves nearer to the trailing edge and the slope of $y(\hat{x})$ at the ends need not be zero.

In subsonic flow, blunt slots with the parameter $\ell/a\,|1-M^2|^{-1/2}$ slightly larger than the value for which convergence could not be obtained exhibited as oscillation of $y(\hat{x})$ very near the trailing edge.

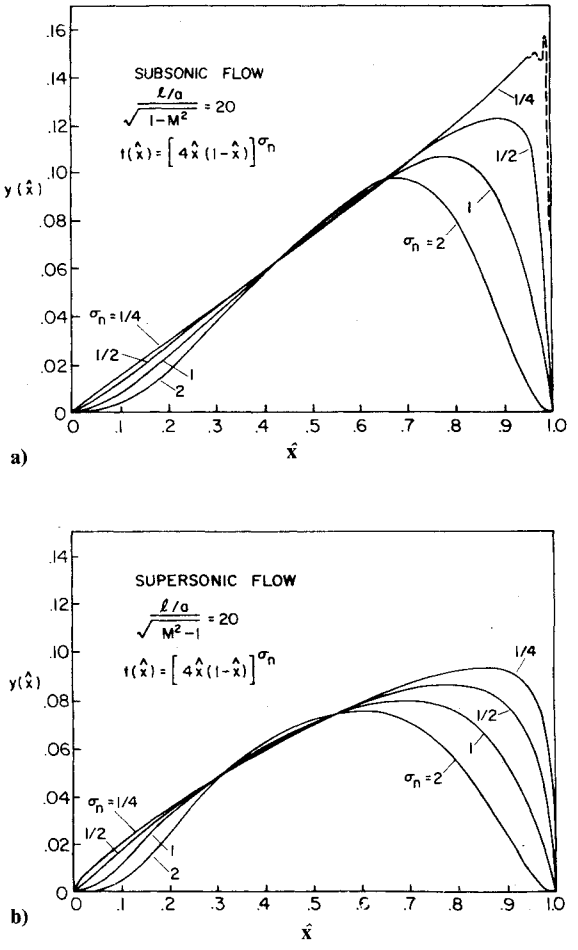

Fig. A1 Typical solutions for $y(\hat{x})$ in a) subsonic flow and b) supersonic flow.

Acknowledgments

The author wishes to thank Prof. E. H. Dowell and Dr. M. H. Williams of Princeton University for their technical advice. The computer programming for the numerical analysis was performed by Todd R. Quackenbush, a Princeton undergraduate. This work was sponsored by the Air Force Office of Scientific Research, Grant 77-3337.

References

[1]Goethert, B. H., *Transonic Wind Tunnel Testing*, Pergamon Press, New York, 1961.

[2]Guderley, G., "Simplifications of the Boundary Conditions at a Wind-Tunnel Wall with Longitudinal Slots," Wright Air Development Center, TR 53-150, 1953.

[3]Baldwin, B. S. Jr., Turner, J. B., and Knechtel, E. D., "Wall Interference in Wind Tunnels with Slotted and Porous Boundaries at Subsonic Speeds," NACA TN 3176, 1954.

[4]Wood, W. W., "Tunnel Interference from Slotted Walls," *Quarterly Journal of Mechanics and Applied Mathematics*, Vol. 17, May 1964, pp. 126-140.

[5]Berndt, S. B. and Sorensen, H., "Flow Properties of Slotted Walls for Transonic Test Sections," *AGARD Conference Proceedings*, No. 174, Paper No. 17, 1975.

[6]Berndt, S. B., "Inviscid Theory of Wall Interference in Slotted Sections," *AIAA Journal*, Vol. 15, Sept. 1977, pp. 1278-1287.

[7]Ashley, H. and Landahl, M. T., *Aerodynamics of Wings and Bodies*, Addison-Wesley, Reading, Mass., 1965.

[8]Pindzola, M. and Chew, W. L., "A Summary of Perforated Wall Wind Tunnel Studies at the Arnold Engineering Development Center," AEDC-TR-60-9, Aug. 1960.